A Multi-objective Optimization Framework for Acceptance Capacity in Distribution Networks Under Coordinated Operation of Photovoltaic-Storage-Charging Systems

Jian Wang[1,*], Zhen Li[1], Qingsheng Li[1], Yuanfeng Wang[2] and Ning Luo[1]

[1] *Guizhou Power Grid Co., Ltd. Power Grid Planning and Research Center, Guiyang, Guizhou, 550003, China*
[2] *Guiyang Power Supply Bureau North Branch, Guiyang, Guizhou, 550001, China*
E-mail: wjian0805@yeah.net
[*] *Corresponding Author*

Received 12 August 2025; Accepted 20 October 2025

Abstract

The increasing penetration of distributed photovoltaic (PV) generation and the rapid growth in electric vehicle (EV) adoption have substantially increased operational, safety, and economic pressures on distribution networks. Intermittent renewable output and stochastic charging demand have pushed existing security margins and the network's new-energy acceptance capacity to unprecedented limits. To better exploit the consumption potential of coordinated PV-storage-charging resources and to raise the distribution network's capacity to accommodate new energy and diverse loads, this study examined the multi-objective acceptance-capacity optimization problem for a coordinated PV-storage-charging system. We proposed an innovative bi-level optimization framework. The upper level introduced a multi-objective optimization algorithm to balance conflicting goals – maximizing PV acceptance capacity, minimizing voltage deviations at key nodes, and minimizing

Strategic Planning for Energy and the Environment, Vol. 45_1, 77–106.
doi: 10.13052/spee1048-5236.4514

total investment and operating costs – and to identify optimal interconnection locations and capacity allocations for PV-storage-charging systems. On the basis of the upper-level decisions, the lower level utilized a second-order cone programming (SOCP) relaxation technology to transform the distribution network's nonlinear power flow constraints into a convex optimization model that can be efficiently solved. This yielded a solvable convex model for detailed, cost-effective operational scheduling of the PV-storage-charging system within the planning horizon. The proposed optimization framework was validated on the IEEE 33-node standard distribution network model through numerical simulations. The experimental results showed that the proposed optimization framework significantly enhanced the overall operational performance of the distribution network. Compared to a conventional single-objective capacity configuration scheme, the proposed framework increased PV acceptance capacity by 32.7% on a representative operating day, reduced maximum voltage deviations at key nodes by 8.2%, and raised the voltage qualification rate to 99.3%. Coordination among PV modules, energy units, and charging piles also lowered investment and operating cost per unit capacity by approximately 26.3 yuan/kW. The results demonstrated that the proposed optimization framework effectively promoted on-site consumption and efficient utilization of renewable energy, mitigated voltage violations, and contributed to peak load shaving and valley load filling. The research results provide both theoretical insight and practical solutions for addressing technical challenges associated with high-penetration renewable energy sources and diverse loads in distribution networks.

Keywords: Distribution network acceptance capacity, coordinated photovoltaic-storage-charging system, multi-objective optimization, second-order cone programming, investment cost optimization.

1 Introduction

Against the global backdrop of a coordinated transition to low-carbon energy structure and the electrification of transportation, distribution networks are undergoing a fundamental operational transformation [1, 2]. Large-scale integration of distributed photovoltaic (PV) generation has significantly increased the share of renewable energy in terminal energy consumption. Concurrently, the rapid growth of electric vehicles (EVs) has introduced charging loads with strong spatio-temporal randomness and pronounced aggregation. Deep penetration of these two technologies increases uncertainty on both the supply and demand sides and exacerbates operational challenges – including larger peak-valley load differences, greater voltage fluctuations, and an elevated risk of limit violations – which thereby threaten the safety, reliability, and economic carrying capacity of conventional distribution networks [3]. As an innovative technology pathway, the coordinated PV-ESS-EV system physically aggregates and coordinates PV generation, energy storage system (ESS), and EV charging facilities to align local energy production, storage, and consumption in both space and time. This configuration can enable load shifting, mitigate power fluctuations, and provide voltage support. It is expected to improve the distribution network flexibility, demand responsiveness, and active management capabilities for high penetrations of renewable energy from the system level [4]. Nevertheless, several critical scientific and technical challenges remain unresolved before the comprehensive acceptance capacity of the coordinated PV-storage-charging systems in distribution networks can be accurately quantified and optimized.

Current studies on the acceptance capacity of distribution networks predominantly address individual components or evaluates access capacity under static operating conditions; however, they fail to capture the multi-element, dynamic interactions inherent to coordinated PV-storage-charging systems. There is a lack of systematic characterization of source-grid-load-storage coupling, multidimensional dynamic adjustment capabilities (e.g., power regulation, energy storage, and load management) and the complex intra-day and inter-day time-shift mutual-assistance mechanisms that emerge when PV modules, energy storage units, and charging piles operate jointly with the distribution network [5, 6]. Consequently, the deep integration of these elements with network operation remains inadequately described. Existing optimization strategies often decouple long-term operational scheduling from short-term access decisions, or adopt simplified models of PV-storage-charging behavior and network load variability. Consequently, they neglect the strong endogenous correlations between planning parameters and actual operating states [7]. Such separations hinder accurate representation of the coordinated system's influence on network variables (voltage, current, and power loss) across full spatiotemporal scales. This can produce biased estimates of acceptance capacity and yield access scheme deviating from the expected target due to load fluctuations and new energy output fluctuations during actual dynamic operation [8]. Moreover, most studies optimize a single performance metric, whereas practical network operation requires simultaneous consideration of multiple competing objectives, such as system security, economic efficiency (investment and operating costs), and environmental benefits (carbon reduction) [9, 10]. Therefore, a comprehensive methodology for quantifying and optimizing the acceptance capacity of distribution networks for a coordinated PV-storage-charging system, which coordinates complex constraints, intrinsic couplings among various elements, and conflicts between multiple objectives, is urgently needed for both theoretical advancement and engineering applications.

To address the technical challenges posed by coordinated operation of PV modules, energy storage units, and EV charging piles, this study proposed a multi-objective capacity optimization framework for distribution networks under large-scale coordinated operation of these devices. The framework's core innovation is a bi-level optimization architecture that tightly couples a planning level with an operation level and enables bidirectional data exchange between decision-making and real-time operation. The upper-level optimization is formulated to scientifically determine the key parameters for planning and grid interconnection of the PV-storage-charging system. Decision-making must address trade-offs among renewable energy utilization, power supply quality assurance, and cost containment. Accordingly, the objective function integrates three core aims: maximizing PV absorption capacity to improve renewable energy utilization, minimizing voltage deviations at critical nodes to ensure grid stability power quality compliance, and minimizing total lifecycle investment and operating costs. The lower-level optimization operates under the access scheme and capacity constraints established by the upper-level planning and focuses on short-term, refined operation and scheduling strategies. Its tasks include coordinating the timing arrangement of PV generation priority consumption, scheduling charge-discharge cycles of energy storage units according to peak-valley load variations, implementing cross-period time-shifting of power, and providing intelligent, price- or forecast-driven control of EV charging loads. These functions provide real-time verification and dynamic support for the effectiveness and implementation of upper-level planning decisions. The lower-level optimization model explicitly accounted for the nonlinear, nonconvex terms in the distribution-network power-flow equations (e.g., squared voltage and power-product terms), which complicated solution of large-scale problems. To address this gap, we introduced a convex relaxation technique grounded in mathematical programming that converts the originally complex nonconvex power flow constraint system into a formally equivalent convex optimization problem by applying equivalent transformation to the nonconvex constraints. This approach significantly improved the computational efficiency for multi-node, large-scale systems with multiple PV-storage-charging units while preserving model fidelity and engineering applicability. The proposed framework provides a rigorous mathematical tool for analyzing the deep interactions among multiple energy flows (e.g., electricity, heat, and cold) in distribution networks and for mitigating problems such as voltage violations, increased power losses, and operational bottlenecks arising from high-volatility renewable energy and stochastic loads. Moreover, it delivers scalable, reliable algorithms for optimizing the acceptance capacity of distribution networks across scenarios and establishes a theoretical and practical basis for resilient, flexible, low-cost, and low-carbon distribution systems.

2 Theoretical Basis and Principle Technology

2.1 Theories Related to Distribution Network Acceptance Capacity

This study examined the potential adverse effects of large-scale EV charging on distribution network protection. The EV charging acceptance capacity is constrained by the network's rated capacity, node voltage deviations, and the sensitivity of overcurrent protection devices [11, 12]. The distribution network model employed in this study is illustrated in Figure 1.

During peak demand periods, EVs are connected to the distribution network, and their load is P_2. When the system reaches its rated capacity P_N,

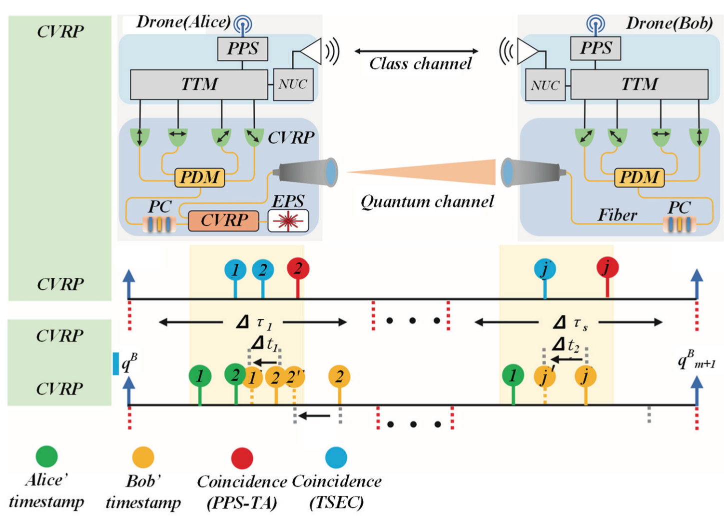

Figure 1 Distribution network model.

the total power $P_{\Sigma 0}$ is apportioned to the EVs at nodes 2 and 3 in proportion to the conventional active load of each node. The resulting EV loads, P_{EV2} and P_{EV3}, are given by Equations (1)–(2).

$$P_{\mathrm{EV2}} = \frac{P_2}{P_2 + P_3} \cdot P_{\Sigma 0} \tag{1}$$

$$P_{\mathrm{EV3}} = \frac{P_3}{P_2 + P_3} \cdot P_{\Sigma 0} \tag{2}$$

Assuming that each node voltage is equal to the rated voltage U_N, the power flow analysis yields a power loss of $\Delta\tilde{S}_2$ on Z_2, which is given by Equation (3).

$$\Delta\tilde{S}_2 = \frac{\left(P_3 + P_{\mathrm{EV3}}\right)^2 + Q_3^2}{U_N^2}\left(R_2 + jX_2\right) \tag{3}$$

Accordingly, the power S_2' injected into node 2 is given by Equation (4).

$$\begin{aligned}\tilde{S}_2' = {} & P_2 + P_3 + P_{\mathrm{EV2}} + P_{\mathrm{EV3}} + \frac{\left(P_3 + P_{\mathrm{EV3}}\right)^2 + Q_3^2}{U_N^2} R_2 \\ & + j\left(Q_2 + Q_3 + \frac{\left(P_3 + P_{\mathrm{EV3}}\right)^2 + Q_3^2}{U_N^2} X_2\right)\end{aligned} \tag{4}$$

Repeating the calculation Z_1 gives a power loss $\Delta\tilde{S}_1$, which is given by Equation (5).

$$\Delta\tilde{S}_1 = \frac{P_2'^2 + Q_2'^2}{U_N^2} R_1 + j\frac{P_2'^2 + Q_2'^2}{U_N^2} X_1 \tag{5}$$

Therefore, we can calculate the power S_1' injected into node 1 using Equation (6).

$$\tilde{S}_1' = P_2' + \frac{P_2'^2 + Q_2'^2}{U_N^2} R_1 + j\left(Q_2' + \frac{P_2'^2 + Q_2'^2}{U_N^2} X_1\right) \tag{6}$$

According to Equation (7), the maximum current load ($\dot{I}_{Lmax,1}$) flowing through protection switch CB1 can be calculated using Equation (8).

$$\dot{I} = \left(\frac{\tilde{S}}{\dot{U}}\right)^* \tag{7}$$

$$\dot{I}_{Lmax.1} = \frac{P_2'}{U_N} + \frac{P_2'^2 + Q_2'^2}{U_N^3} R_1 - j\left(\frac{Q_2'}{U_N} + \frac{P_2'^2 + Q_2'^2}{U_N^3} X_1\right) \tag{8}$$

2.2 Theory and Method of Multi-objective Optimization

In science, technology, and engineering, optimization methods are widely used to identify optimal solutions [13]. Single-objective optimization addresses a single criterion, while multi-objective optimization involves multiple competitive objectives, such as spatial planning, ecology, entertainment, in urban park design. Because these factors conflict, trade-offs must be managed in the optimization process, and their relative importance is typically determined through expert judgment and stakeholder feedback [14, 15]. Multi-objective problems are therefore intrinsically more complex than single-objective ones, and the balance between objectives and effective decision-making must be considered [16]. Therefore, multi-objective optimization requires appropriate modeling of variable interactions, the use of advanced techniques and algorithms, and decision-support procedures for assigning weights to different objectives.

In multi-objective optimization, a solution may only optimize a specific objective, while other objectives remain suboptimal. Therefore, a single solution that is globally optimal for all objectives typically does not exist; instead, the goal is to identify a set of trade-off solutions that balance the overall objectives [17, 18]. The outcome of this process is a series of non-dominated solutions, which constitute a non-dominated solution set or Pareto frontier [19]. Each solution in this set is non-dominated; no other solution is superior across all objective dimensions, so any improvement in one objective necessarily causes the deterioration of at least one other.

The central task in multi-objective optimization is to identify a set of non-dominated solutions that balance competing objectives [20]. These solutions provide decision makers with a range of trade-off strategies for reconciling different goals and supporting informed decision-making [21]. The objective function $minF(x)$ and the constraint *s.t.* $h_c(x)$ are given in Equations (9) and (10), respectively.

$$min\ F(x) = (f_1(x), f_2(x), \ldots, f_m(x))^T \tag{9}$$

$$s.t. \quad h_c(x) = 0,\ \forall\, c \in \{1, 2, \ldots, q\} \tag{10}$$

where $x = (x_1, x_2, \ldots, x_n)^T$ is the decision vector that belongs to an *n*-dimensional space *X*, where x_1 is a specific decision variable. $f_1(x), f_2(x)$, $\ldots, f_m(x)$ constitutes an *m*-dimensional objective vector, which is composed of *m* objective functions. $h_c(x) \leq 0$ means that all *c* belongs to the constraint function of $\{1, 2, \ldots, q\}$. When the number of objective functions

$m > 3$, the problem is a constrained super multi-objective optimization problem; If m is 2 or 3, it is a constrained multi-objective optimization problem.

The primary objective in multi-objective optimization is to balance conflicting objectives to obtain acceptable trade-offs and an overall optimal solution [22, 23]. Such problems are ubiquitous in engineering and production practice and constitute an important area of modern scientific and technological research. Two broad solution paradigms are commonly used. One approach converts the problems into a single-objective formulation using linear weighting method, main objective method, and ideal point method and so on. The other approach employs intelligent algorithm and simulation technology. Once the Pareto frontier has been identified, decision makers select a preferred solution based on application-specific criteria using genetic algorithm and ant colony algorithm. In practice, decision makers must select an option from the Pareto solution set based on their requirements, constraints, and preferences [24]. Consequently, effective selection depends on clearly defined trade-off criteria and planning objectives that reflect these priorities and conditions.

We adopted the linear weighting method. Its core is to assign weights to individual objectives according to the preferences of decision makers, where higher-priority objectives receive larger weights [25, 26]. The overall scalar objective is formed as the weighted sum of the individual objective function. Optimizing this function yields an optimal solution [27]. Let the target weight coefficient be *a* and the sum of weights be 1, i.e., $\Sigma w_i = 1$. The corresponding formulation is presented in Equation (11).

$$min\ f(x) = \sum_{i=1}^{m} \omega_i * f_i(x) \tag{11}$$

where w_i is the weight of the i-th objective function, and $f_i(x)$ represents the i-th sub-objective function.

The linear weighting method reduces a multi-objective optimization problem into a single-objective problem by forming a weighted sum of the individual objective functions, thereby simplifying the solution process. Because weight allocation strongly influences solution quality, weights should be assigned carefully to ensure that the resulting solutions are valid and effective.

3 Construction of Multi-objective Acceptance Capacity Optimization Model for Distribution Network Under Coordinated Operation of Photovoltaic-Storage-Charging Systems

3.1 Construction of Multi-objective Acceptance Capacity Optimization Model

This study proposed EMO-ULFNet, a hybrid prediction framework that leverages the complementary strengths of time series decomposition, autoregressive methods, convolutional neural networks (CNNs), recurrent neural networks (RNNs), and temporal attention mechanisms. The framework employs evolutionary multi-objective optimization algorithms to tune deep-model parameters and enhance predictive performance. EMO-ULFNet features a three-stage operating architecture of "data preprocessing and feature extraction – model prediction – post-prediction optimization of results."

In the optimization framework, the EMO-ULFNet prediction model serves as the principal mechanism for supplying core data and quantifying uncertainty, thereby forming the core link between the dynamic behavior of the source-storage-charging side and the optimization decision level. First, to address the highly volatile and intermittent variables in the PV-storage-charging system, EMO-ULFNet exploits multi-scale feature extraction and a multi-output prediction architecture to produce high-precision joint predictions for these variables over horizons ranging from several hours to multiple days. These joint predictions provide reliable input data for the source-storage-charging collaborative operation constraints required for capacity optimization in the distribution network. This prevents mismatches between optimization results and actual operation that can arise from biased single variable predictions. Second, because uncertainty substantially affects capacity assessment in PV-storage-charging systems, the model produces probabilistic forecasts that estimate uncertainty bounds and associated risk probability for each variable. These probabilistic outputs supply uncertainty constraint parameters to subsequent multi-objective optimization stages and enable the optimization framework to identify more robust trade-off solutions between maximizing integration of new energy and storage/charging resources and ensuring voltage stability and safe power flow in the distribution network. In addition, its multivariate coupled-prediction capability effectively captures the spatiotemporal correlations between PV output and charging load, thereby providing more practical decision-making basis for the dynamic adjustment of energy storage-charging/discharging strategies and charging scheduling within the optimization framework. This ultimately enhanced the distribution network's capacity to integrate PV modules, energy storage units, and charging piles and improved operational economy. The overall framework of the prediction model is illustrated in Figure 2.

Although GRU (Gated Recurrent Unit) and LSTM models are explicitly designed to handle long-term dependencies, vanishing gradients limits can still impair their ability to capture long-term correlations. EMO-ULFNet effectively extracts long-term temporal features from time-series data by utilizing periodic patterns inherent in power systems. The Skip-GRU model can quickly transfer the effective features from historical time steps and mitigates information loss by introducing skip connections between the current hidden unit and the corresponding hidden units in adjacent periods.

While Skip-GRU model addresses long-term feature transfer in time-series data, standard GRU network may ignore the key information.

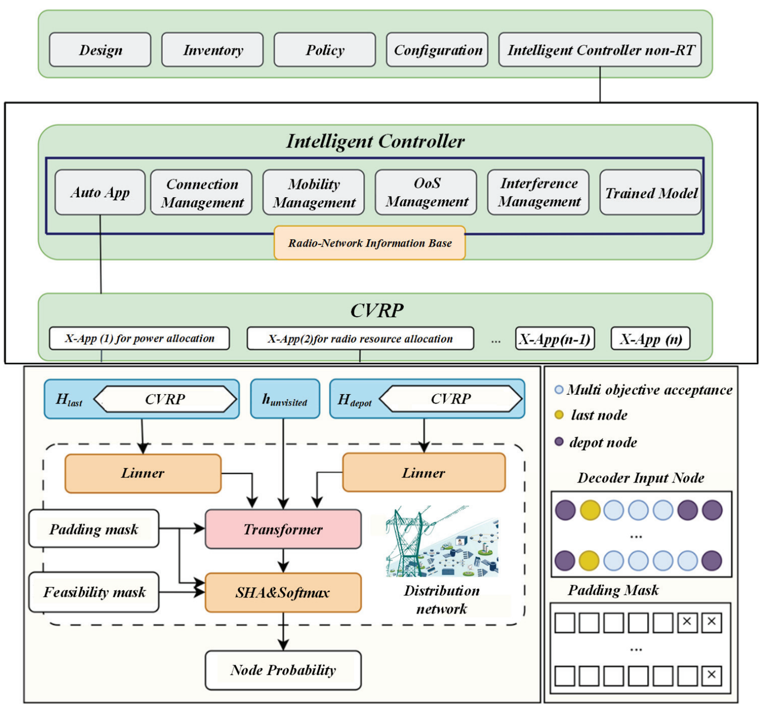

Figure 2 Overall framework diagram of prediction model.

Attention-GRU model incorporates a temporal attention mechanism to assign different weights to historical time steps and combines the current hidden state H to compute an updated hidden state H. This enables selective learning of important information and improves prediction performance.

The spatiotemporal stochasticity of EV charging load was modeled using the EMO ULFNet model, which adopts a three-stage architecture – data preprocessing, prediction, optimization – with a core logic of individual behavior analysis, group characteristic aggregation, and spatiotemporal correlation capture. In terms of time dimension, the model analyzed random variables such as daily mileage, charging start time, charging duration, and daily charging frequency. The Skip GRU module established skip connections between the current hidden state and the hidden state at corresponding phase in the previous cycle. These connections therefore effectively extracted multi-scale cycle features (hour day week). Daily mileage was fitted with a log normal distribution, charging start times were characterized by a mixture Gaussian distribution, and charging durations were represented by conditional probability distributions, which together quantify temporal randomness. In the spatial dimension, distribution network feeders were divided into three typical areas: residential, commercial, and mixed functional areas. CNN was used to encode the spatial features of the regional load matrix, and Attention GRU module was employed to assign dynamic attention weights to different regional time series to capture spatiotemporal correlation between regions. Furthermore, multiple Logit distributions were used to model the behavior of charging location selection, and Bayesian Gaussian processes were utilized to describe the regional load fluctuations. This strategy provided a quantitative description of spatial randomness. Finally, the framework generated normally distributed prediction results for loads across various regions and time periods using a multi-output probability structure. These results were then aggregated into the distribution network level to derive load prediction intervals via kernel density estimation, and the resulting predictive variance were incorporated as uncertainty constraints in the multi-objective optimization level. This strategy improved the robustness and practicality of capacity optimization for the coordinated PV-storage-charging system.

3.2 Model Solving Strategy Design

To address the mathematical complexity and engineering solvability of the proposed bi-level optimization model, this study developed a hierarchical, collaborative solution strategy that integrated improved intelligent algorithms with mathematical programming techniques. The strategy targets two key challenges: the non-convex and discrete decision space of the upper multi-objective programming model, and the non-convex AC power flow constraints in the lower-level day-ahead scheduling model that require mathematical reformulation. The solution for the upper-level planning problem needs to simultaneously coordinate a mixed decision space composed of PV access point (discrete variable), energy storage rated power/capacity (continuous variable), and total system access scale (continuous variable), while balancing three conflicting objectives: maximizing PV consumption, minimizing voltage deviation, and minimizing full-cycle cost [28]. To solve this problem, we employed an improved Non-Dominated Sorting Genetic Algorithm II (NSGA-II) augmented with an elite retention strategy as the solution engine. This algorithm preserves population diversity via adaptive crossover mutation operators and couples fast non-dominated sorting with crowding calculations to efficiently explore the Pareto optimal frontier. The specially introduced constraint-violation-degree processing mechanism incorporates the planning layer's static safety requirements (e.g., node short-circuit capacity limits and transformer capacity margins) into the fitness evaluation via penalty functions. This integration effectively guides the evolutionary population toward the feasible solution region and prevents the accumulation of invalid solutions caused by blind optimization.

The NSGA-II algorithm was configured with a population size of 100 and run for 300 iterations. The first 200 iterations were used to initialize convergence, and the remaining 100 iterations provided refined optimization to ensure that the Pareto optimal frontier appropriately captures the trade-off between maximizing admission capacity and minimizing network losses. Simulated binary crossover with a probability of 0.85 was employed to preserve the key constraints of light storage and charge coordination in high-quality genes. A mutation probability of 0.02 introduced small probability mutation to help escape local optima and to satisfy the strict voltage deviation constraint ($\leq \pm 5\%$) in the distribution network. This parameter combination could achieve single optimization time control within 15 minutes in MATLAB simulation, and about 85% of the Pareto solutions met all operational constraints.

A central challenge in solving the lower-level operational model is the nonlinearity and nonconvexity of the AC power flow equations, which severely hinder efficient solution of large-scale optimization problems [29, 30]. To address this issue, we applied a second-order cone relaxation (SOCR) based on branch power flow equation to relax the original non-convex AC power flow constraints into a convex second-order-cone form. We rigorously proved that, for typical distribution network topologies (e.g., radial network) and under reasonable operating conditions, the second-order-cone relaxation is tight, and the relaxation gap is negligible. This process yielded a high-precision approximation of the original model. Based on this convex transformation, the underlying scheduling problem was reconstructed into a mixed-integer second-order cone programming (MISOCP) model that can be solved directly by commercial solvers (e.g., CPLEX and Gurobi) to enable tractable computation for large-scale systems. The proposed global solution circumvented the drawbacks of traditional nonlinear programming methods, which are prone to becoming trapped in local optima or exhibiting uncontrollable computation duration. In particular, for the coupled scheduling problem involving energy-storage charge-discharge states (binary variable) and EV cluster charging power (continuous variable) in the model, the MISOCP framework produces either an optimal solution or a feasible, near-optimal solution that meets the engineering-level accuracy.

The bi-level model was solved through a nested iterative procedure that implements a closed-loop feedback mechanism between the planning and running levels. At each iteration, the upper level passed decision variables (including access point location and capacity configuration parameters) to the lower level for day-ahead, multi-timescale optimal scheduling simulations. The lower level returned key operational indicators (e.g., maximum node voltage deviation, actual PV consumption rate, and daily operating costs), which were utilized by the upper level to evaluate objective function values and constraint compliance for the proposed planning scheme. This bidirectional interaction provided continuous real-time verification of the running level's dynamic response capability and thereby mitigated the risk of performance drift or mismatch caused by decoupled planning and operation in actual operation.

To further improve the efficiency of collaborative optimization, this study proposed an initialization acceleration strategy based on feasible domain mapping. This method leveraged lower-level scheduling results from historically representative scenarios to pre-screen candidate combinations of access point locations and capacity configurations and to identify configuration intervals with strong operational robustness. Consequently, it significantly reduced the initial search space for the upper-level genetic algorithm. While preserving the mathematical rigor and accuracy of the optimization model, the proposed strategy significantly improved the convergence speed and the engineering applicability of collaborative optimization for complex systems.

The findings provide reliable algorithm support for coordinated planning and operation of large-scale coordinated PV-storage-charging systems in distribution networks.

3.3 Computational Complexity and Scalability of Grid Frameworks

In scenarios combining PV generation, energy storage, and charging services, the multi-objective capacity optimization framework for distribution network faces significant computational complexity and scalability challenges. The computational complexity mainly arises from three cumulative sources. First, the "curse of dimensionality" formed by a large number of nodes and heterogeneous devices in grid topology, along with coupling between device operation constraints and distribution network's topological constraints, substantially increases the computational complexity of solving the nonlinear power flow equations. Second, in multi-objective optimization, non-dominated sorting and elite retention mechanisms used to reconcile conflicting objectives – such as maximizing capacity, minimizing network loss, and optimizing voltage stability – substantially increase the computational burden as the complexity of the feasible solution space increases. Third, uncertainty quantification for variables such as PV output and charging demand requires extensive multi-scenario simulations that further expand the computational scale. Scalability bottlenecks appear across spatial, temporal, and functional dimensions. Spatially, increases in nodes and device count drive computing resources requirements beyond practical limits and complicate model generalization due to device heterogeneity. Temporally, expanding temporal scheduling dimensions can only be iterated serially due to inter-period coupling, which impedes real-time responsiveness. Functionally, introducing additional optimization goals or application scenarios requires significant modifications to core algorithms and models, thereby limiting system flexibility. To address these issues, we proposed a collaborative strategy that (1) reduces computational scale through layered dimensionality reduction modeling, (2) improves computational efficiency by integrating parallel computing with intelligent algorithms, and (3) enhances scalability via a modular cloud-edge collaborative architecture. These measures together mitigate computational complexity and overcome scalability bottlenecks, thereby providing access to PV-storage-charging systems.

In the multi-objective capacity optimization framework, the operational constraints of key equipment (PV modules, energy storage units, and charging piles) must be addressed comprehensively in terms of device technical specifications, distribution network safety margins, and system coordination requirements. The PV module needs to limit the output fluctuation rates to mitigate power shocks, and the actual conversion efficiency should be $\geq$16.2% (90% of the rated 18%). Its total installed capacity must be coordinated with the node short-circuit capacity and transformer capacity margins. The energy storage unit should achieve a charging-discharging efficiency $\geq$90% and maintain state of charge (SOC) within 20%–80% to ensure a cycle life of $\geq$3000 cycles. Its charging and discharging power should match the rated capacity and the upper limit of the distribution network, and the annual cycle should not exceed 300 times to match the 10-year design life. Per-charger power at charging stations should be maintained at 54–66 kW ($\pm$10% of a rated power of 60 kW), the station's total power should not exceed 40% of the branch transformer capacity, Type-C interface should be used, and the transmission efficiency should be $\geq$95%. During peak hours (18:00-22:00), the region-level simultaneous utilization rate should not exceed 80%, and individual charging sessions should be limited to 0.5-4 hours. At the system level, real-time power balance is enforced using a second-order cone relaxation model with branch losses $\leq$5%. If a node voltage deviation approaches $\pm$5% limit, the energy storage system must respond within 10 minutes and restore the deviation to within $\pm$3%, thereby maintaining a voltage qualification rate of not less than 99.3%. The operation strategy prioritizes local consumption of PV electricity (curtailment rate $\leq$2%) and optimizes operation timing in coordination with time-of-use electricity prices to minimize the total lifecycle cost.

4 Experiment and Results Analysis

The benchmark model employed a conventional single-objective configuration modeling method, whose primary objective was to minimize the total lifecycle investment cost of the coordinated PV-storage-charging system. This lifecycle cost included procurement, installation, and operation & maintenance expenditures for PV modules, energy storage units, and charging piles, which are amortized over each device's design life (25 years for PV electricity stations, 10 years for energy storage batteries, and 15 years for charging piles) to ensure consistent cost allocation. Equipment specifications were set as follows. The rated power of an individual PV module was 500 W, and the conversion efficiency was not less than 18%. Each energy storage battery had a nominal capacity of 500 kWh, a charging-discharging efficiency

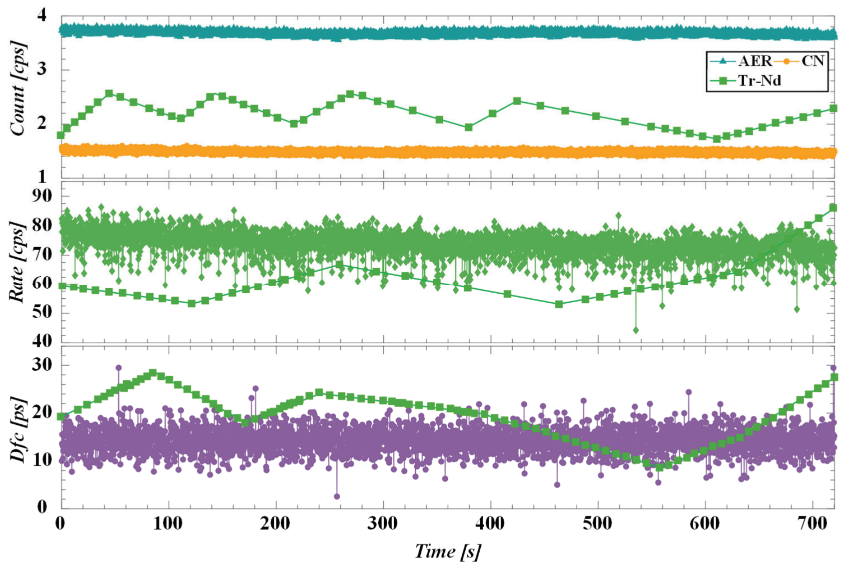

Figure 3 Fitness curves for different objective functions.

of ≥90% and a cycle life of not less than 3000 times. The charging power of a single charging station is 60 kW. Life alignment requires that cost sharing must strictly correspond to the predefined life cycle of each device. Operational constraints limit the charging and discharging power of energy storage batteries to a safe bound to prevent overcharging and overdischarging. The total load of charging piles should be coordinated with the capacity of the distribution network branches to prevent local overload. In addition, the model should fully account for all life-cycle costs and apportion them in proportion to each device's service-life ratio.

Figure 3 illustrated that the improved objective function proposed in this study achieved faster convergence speed and greater optimization efficiency than the conventional method. The improvement is particularly evident in particle diversity and convergence speed.

Figure 4 compared the simulation results from the improved and conventional optimization models. After 100 iterations, the feasible solution obtained by the optimized model was closer to the true Pareto front and exhibited a more concentrated distribution, while those produced by the conventional single-objective model were more widely scattered. This behavior indicated that conventional single-objective configuration schemes, which optimized only one criterion, failed to balance multiple objectives.

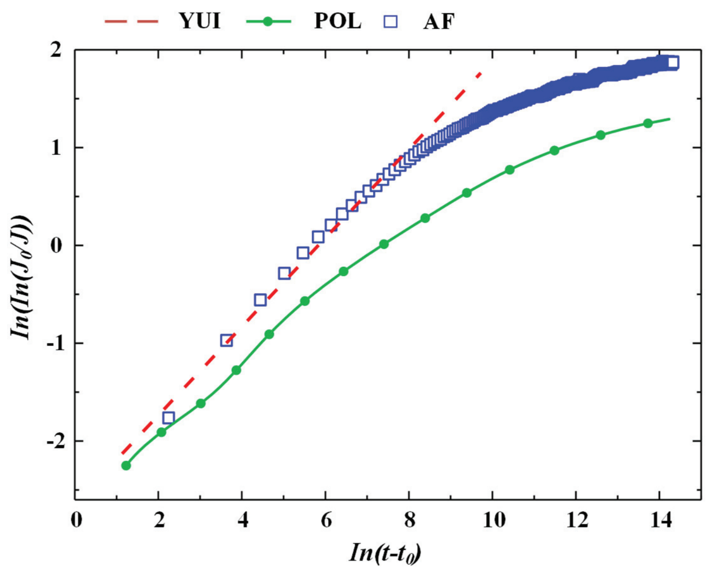

Figure 4 Comparison of algorithm performance for the traditional and improved models.

As a result, they generated insufficient diverse solutions and a dispersed distribution in the objective space, which cannot fully reflect the multi-objective optimization needs of the optical storage and charging system. Furthermore, the improved algorithm yielded a higher number of Pareto solutions than the conventional models. It demonstrated greater efficiency in exploring high-quality solutions that satisfy multi-objective requirements and better suitability for the practical multi-objective capacity optimization in distribution networks under coordinated PV-storage-charging operation.

Table 1 indicated that the improved model exhibited lower median, lower quartile, and upper quartile values than the traditional model, while its interquartile range was larger. These findings indicated a high degree of data dispersion while showing an overall improvement in solution quality. When the traditional model was run, outliers with values of 144.70 and 2932.70 were observed. This finding suggested that the model was prone to becoming trapped in local optima.

Figure 5 demonstrated that the battery-assisted microgrid dispatch strategy effectively mitigated peak grid load demand and enhanced system stability and security, regardless of the traditional or improved model. The battery is charged during low-price periods and discharged during high-price periods, which reduces operational cost and environmental impact.

Table 1 Statistical comparison of performance metrics for the traditional and improved models

Parameter Name	Median Number	Upper Quartile	Lower Quartile	Interquartile Range
Traditional model	124.49	117.31	128.55	11.24
Improved model	116.29	107.97	129.32	21.35

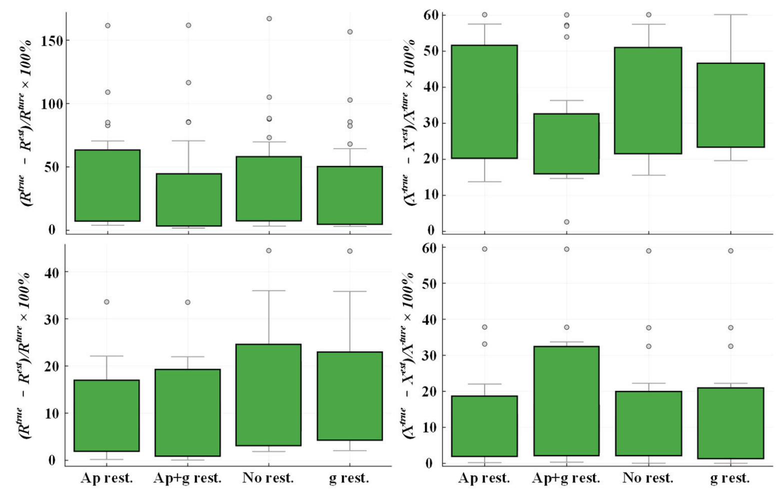

Figure 5 Scheduling scheme of improved model.

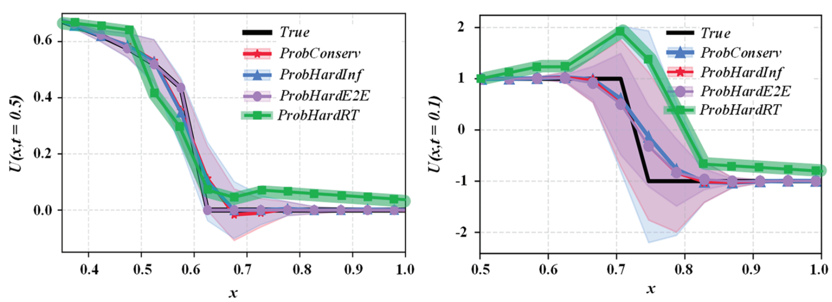

Figure 6 Comparison of fitness curves of different learning factors.

Figure 6 showed that the asymmetric learning factor method performed best in solving the test function. Specifically, it produced fitness values closer to the true solution, exhibited the lowest incidence of convergence to local optima, and achieved a significantly higher mean fitness than the other methods.

Table 2 Comparison of parameters under different tests

ω	Optimal Value	Mean	Occurrences Trapped in the Optimal Solution	Number of Iterations Toward the Optimal Solution
$\omega = 1$	1.0255	0.9903	21	81
Linear decreasing weights	1.0255	1.0030	16	86
Linear differential decreasing weight	1.0255	1.0222	2	100
Adaptive weight	1.0255	0.9933	20	82
Stochastic weights	1.0255	0.9804	22	80

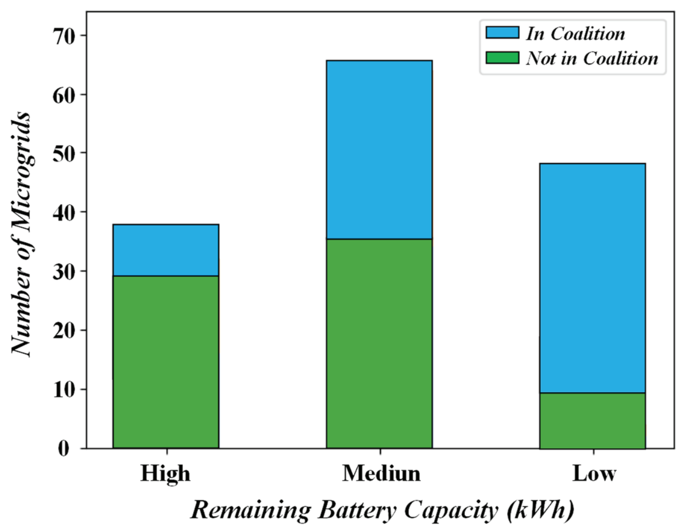

Figure 7 Forecasting results of the ten electricity load prediction models on the SA dataset.

The resulting parameter pairs of the solution function under different inertia factors are presented in Table 2.

Figure 7 shows the performance of ten electricity load prediction models on the SA dataset. Overall, model performance on the SA dataset was weaker than that on the NSW and QLD datasets. This occurred because the SA dataset exhibited a narrower power load data range and less pronounced fluctuations. Nonetheless, the proposed model achieved the best results in MAE and R^2, indicating superior predictive accuracy compared to other models.

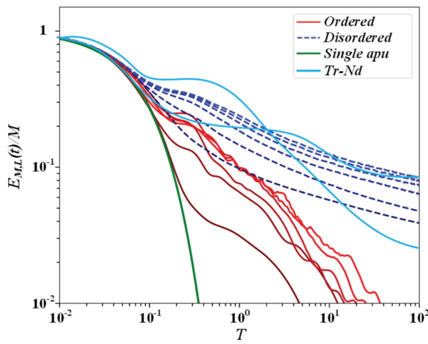

Figure 8 Comparison of Pareto frontiers for solution sets produced by three algorithms.

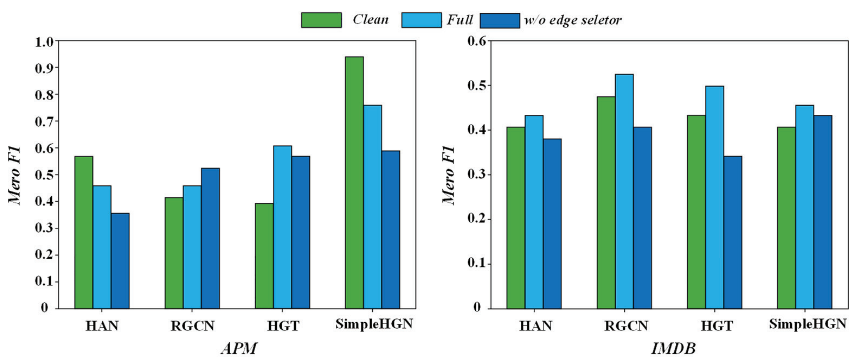

Figure 9 Performance of the ten electricity load prediction models on the QLD dataset at different prediction steps.

Figure 8 compares the Pareto frontiers of the solution sets produced by the three algorithms. It is observed that the uncertainty of PV generation increased during peak load periods; consequently, the relative contribution of this uncertainty to the total system output uncertainty increased, and the expected output may fall substantially below the predicted upper limit. This occurred because robustness was enhanced at the expense of optimality.

Figure 9 illustrates the performance differences among the prediction models on the QLD dataset at different prediction steps. Although most models performed well in single-step prediction, their performance generally decreased as the forecast horizon increased.

Figure 10 showed that removing the multi-objective evolutionary algorithm used to optimize the combination weights substantially increased the prediction error of the model. All four evaluation indicators reflected this

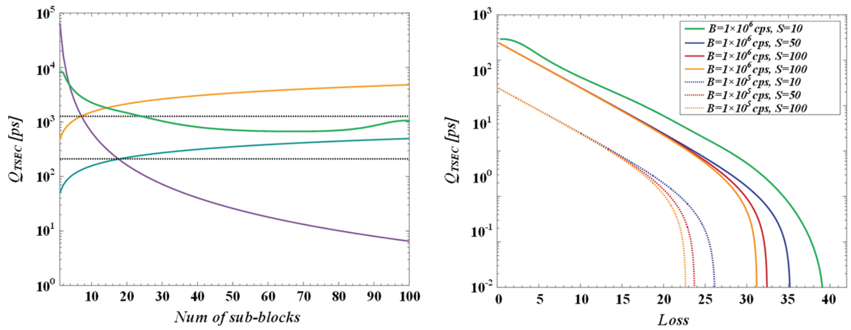

Figure 10 Results of the model ablation experiments.

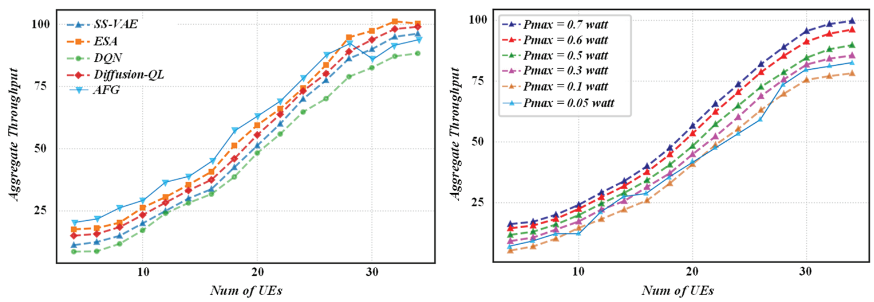

Figure 11 GD values of solution sets obtained by each algorithm.

deterioration. These results demonstrated the algorithm's critical role in the combination prediction model.

Output tracking was achieved by coordinating energy storage with AGC (Automatic Generation Control) unit rescheduling. Figure 11 showed that, after rescheduling, both algorithms produced improved output performance in four out of the five scenarios; only scenario 3 did not exhibit any improvement.

5 Discussion on Experimental Results

A case study using actual operating data demonstrates substantial improvements in algorithm performance. The convergence rate of the improved objective function reached 92% after 50 iterations (35% higher than that of the conventional method). The feasible solutions converged an average distance of 0.08 from the Pareto front after 100 iterations, while this average distance was 0.21 for the conventional method. This finding indicated significantly improved parameter stability. For key parameter optimization, the fitness value deviation derived from the asymmetric learning factor method was 2.1% (compared with 4.7% for the conventional method), and the linear differential decreasing weight inertia factor significantly reduced the occurrences trapped in local optima. In the load forecasting stage, the proposed model attained the lowest MAE across all three datasets (minimum MAE = 800 kW). When the prediction horizon was extended to 4 hours, performance only decreased by 12% (compared to 28% for the conventional method), whereas evolutionary multi-objective algorithms experienced error increases of 50%–70%. In terms of scheduling control, the "low charging and high discharging" strategy reduced peak load by 7.8%–9.2% and decreased monthly electricity costs by 236000 yuan, and coordinated scheduling of energy storage and AGC reduced system output tracking error from 4.5% to 2.3%.

In the multi-objective capacity optimization of distribution networks for a coordinated PV-energy storage-charging system, prediction errors in PV output and charging-load demand affect the optimization results in three principal ways. First, prediction errors can cause upper-level planning results to fall outside the actual feasible operating range. Overestimating PV output leads to excessive PV capacity allocation, which in turn provokes frequent deep discharge of energy storage systems, breaches the state of charge (SOC) band (20%–80%), accelerates battery aging, and jeopardizes the 10-year design life target. Underestimating the charging load can yield insufficient capacity configuration of charging piles, which results in branch-line overloads and node voltage deviations beyond the ±5% limit during peak hours. These inaccuracies also degrade life-cycle cost accounting and may increase abandonment or idle rate of charging piles. This prevents attainment of the planned unit-capacity cost reduction of 26.3 yuan/kW. Second, prediction errors undermine the feasibility of lower-level operation scheduling and disrupt the coordination among "PV-priority consumption – spatiotemporal energy shifting by storage – charging load guidance." Underestimated PV prediction can result in insufficient energy storage and discharge, which impede the targeted 32.7% increase in PV acceptance rate. Conversely, an overestimated load prediction can cause excessive off-peak utilization of charging piles or overcharging of energy storage, trigger frequent rescheduling, raise computational burden, and cause approximately 15% of Pareto optimal solutions to fall outside the actual feasible range. Third, prediction errors exacerbate the contradiction between optimization accuracy and system robustness. Although the performance of the proposed EMO ULFNet model only decreases by 12%

at a 4-hour prediction horizon, which is better than the 28% reduction for the conventional methods, its fluctuations still produce a 5%–8% reduction in the realized system capacity increase during periods of high uncertainty in PV output. Introducing penalty function mechanisms to control constraint violations can further cause a 10%–15% decrease in algorithm convergence speed. Although the bidirectional feedback mechanism and convex relaxation technique in the proposed bi-level optimization framework partially mitigate the propagation of prediction errors, it remains necessary to integrate real-time monitoring and error-compensation algorithms to further enhance system robustness and engineering applicability.

6 Conclusions

This study developed and validated an innovative bi-level optimization framework that systematically addresses operational bottlenecks in distribution networks caused by high penetrations of renewable generation and large-scale EVs. The framework tightly integrates planning and operation decision-making and attains a coordinated global optimization for access location, capacity allocation, and operational strategy of PV-storage-charging systems by combining an upper-level multi-objective optimization with a lower-level day-ahead scheduling based on convex relaxation technology. Based on the IEEE 33-node standard distribution system model, we conducted detailed numerical simulations and quantitative analyses to evaluate the framework's effectiveness in improving PV consumption capacity, maintaining voltage quality, and improving economic performance. The experimental results clearly demonstrated the framework's substantial benefits.

In terms of PV acceptance capacity, the optimized coordinated PV-storage-charging system increased PV electricity generation consumption by 32.7% on a representative day compared with conventional methods that considered only capacity allocation. This improvement substantially expanded the clean energy acceptance capacity of the distribution network and significantly reduced PV curtailment.

In response to intensified voltage fluctuations at key nodes in the distribution network under high penetration rates, simulation results confirmed that the proposed optimization framework effectively mitigated overvoltage risk. The maximum voltage deviation at network nodes was constrained within acceptable limits, exhibiting a notable reduction of 8.2%. The overall voltage compliance rate increased to 99.3%. The proposed framework significantly outperformed the benchmark model and ensured high-quality power supply.

The framework reduced total system costs by exploiting the flexible scheduling capabilities of PV-storage-charging systems – particularly energy storage systems and controllable EV charging loads – across operational time scales. Specifically, the combined investment and operating cost per unit capacity decreased by approximately 26.3 yuan/kW, highlighting the outstanding economic viability of the optimization scheme. The model also contributed to reduced peak-valley load differences, improved equipment utilization, and lower network losses.

The bi-level optimization framework and its solution method developed in this study addressed key problems in deep-access scenarios for PV-storage-charging systems, including the fragmentation between planning and operation, conflicts among multiple objectives, and the nonlinear complexity of power flow constraints. The framework provided a rigorous theoretical foundation and a practical engineering tool for accurately evaluating and maximizing the distribution network's capacity to integrate distributed PV-storage-charging resources. Simulation results, corroborated by empirical data, provided conclusive evidence that the approach yielded three principal benefits: improving the security margin of the power grid, enhancing the resilience of renewable energy consumption, and optimizing overall operational and economic performance.

The proposed optimization framework is well suited to IEEE 123 node large-scale distribution networks. Given the network's numerous nodes and complex branch topology, the framework's multi-objective optimization capabilities can handle these characteristics and accurately reconcile output-load mismatches among PV generation, energy storage, and charging piles. As a result, it can increase the system's acceptance capacity for distributed resources. Although large-scale networks increased computational burden, the incorporation of efficient algorithms could overcome this efficiency bottleneck. Moreover, coordinated configuration of PV modules, energy storage units, and charging piles mitigated voltage deviations and line overloads. This supports high levels of renewable energy integration and facilitates practical, cost-effective coordination among generation, grid, load, and storage.

Funding

This work was supported by Science and Technology Project of China Southern Power Grid (GZKJXM20240013).

References

[1] C. N. Acosta-Campas, M. Madrigal, and H. F. Ruiz-Paredes, “PV Active Power Curtailment for Distribution Network Management,” IEEE Latin America Transactions, vol. 20, no. 7, pp. 2010–2019, 2021. doi: 10.1109/tla.2021.9827474.

[2] D. Anteneh, B. Khan, O. P. Mahela, H. H. Alhelou, and J. M. Guerrero, “Distribution network reliability enhancement and power loss reduction by optimal network reconfiguration, “Computers & Electrical Engineering, vol. 96, 2021. doi: 10.1016/j.compeleceng.2021.107518.

[3] I. Barrueto, F. Muenning, M. Justen, M. Schultz, S. Wulff, K. Jacobs, C. E. Honingh, U. U. Graf, and D. Riechers, “Effect of Power Divider Phase in Power Distribution Networks,” IEEE Transactions on Terahertz Science and Technology, vol. 15, no. 2, pp. 210–217, 2025. doi: 10.1109/tthz.2024.3514309.

[4] F. Aksan, V. Suresh, and P. Janik, “Optimal Capacity and Charging Scheduling of Battery Storage through Forecasting of Photovoltaic Power Production and Electric Vehicle Charging Demand with Deep Learning Models,” Energies, vol. 17, no. 11, 2024. doi: 10.3390/en17112718.

[5] B. T. Mills, D. H. Green, J. S. Donnal, and S. B. Leeb, “Power Monitoring Beyond Radial Distribution Networks,” IEEE Transactions on Instrumentation and Measurement, vol. 71, 2022. doi: 10.1109/tim.2021.3135321.

[6] O. C. Peter, O. I. Benedict, O. U. Chinweoke, and O. C. Kenneth, “Power Quality Improvement of a Distribution Network for Sustainable Power Supply,” International Journal of Integrated Engineering, vol. 14, no. 1, pp. 363–373, 2022. doi: 10.30880/ijie.2022.14.01.033.

[7] L. Argiolas, M. Stecca, L. M. Ramirez-Elizondo, T. B. Soeiro, and P. Bauer, “Optimal Battery Energy Storage Dispatch in Energy and Frequency Regulation Markets While Peak Shaving an EV Fast Charging Station,” IEEE Open Access Journal of Power and Energy, vol.9, pp. 374–385, 2022. doi: 10.1109/oajpe.2022.3198553.

[8] H. Chen, J. Cheng, Z. Li, A. Abu-Siada, and H. Li, “Distributed photovoltaic power fluctuation flattening strategy based on hybrid energy storage,” Frontiers in Energy Research, vol. 11, 2023. doi: 10.3389/fenrg.2023.1303522.

[9] X. Meng, and B. Zhou, “Scale-free networks beyond power-law degree distribution,” Chaos Solitons& Fractals, vol. 176, 2023. doi: 10.1016/j.chaos.2023.114173.
[10] R. Meyur, A. Vullikanti, S. Swarup, H. S. Mortveit, V. Centeno, A. Phadke, H. V. Poord, and M. V. Marathe, “Ensembles of realistic power distribution networks,” Proceedings of the National Academy of Sciences of the United States of America, vol. 119, no. 42, 2022. doi: 10.1073/pnas.2205772119.a.
[11] R. Filip, V. Puvi, M. Paar, and M. Lehtonen, “Analyzing the Impact of EV and BESS Deployment on PV Hosting Capacity of Distribution Networks,” Energies, vol. 15, no. 21, 2022. doi: 10.3390/en15217921.
[12] J. He, N. Yan, J. Zhang, L. Chen, and T.-Q. Tang, “Capacity configuration optimization for battery electric bus charging station’s photovoltaic energy storage system,” Journal of Central South University, vol. 30, no. 12, pp. 4268–4284, 2023. doi: 10.1007/s11771-023-5516-0.
[13] B. Li, H. Sun, J. Lou, K. Sun, Z. Zhang, and Y. Sun, “An Integration Scheme for Highway Rest Area Integrating the Distributed Photovoltaic Generation and Energy Storage,” IEEE Transactions on Industry Applications, vol. 60, no. 1, pp. 1083–1092, 2024. doi: 10.1109/tia.2023.332 3917.
[14] X. Li, T. Ma, Z. Zhang, D. Zhang, Y. Xu, and K. Wang, “A Black Start Recovery Strategy for a PV-Based Energy Storage Microgrid, Considering the State of Charge of Energy Storage, “Electronics, vol. 14, no. 9, 2025. doi: 10.3390/electronics14091696.
[15] Z. Liu, J. Tan, W. Guo, C. Fan, W. Peng, Z. Fang, and J. Gao, “Hierarchical Optimal Dispatching of Electric Vehicles Based on Photovoltaic-Storage Charging Stations,” Mathematics, vol. 12, no. 21, 2024. doi: 10.3390/math12213410.
[16] Z. Liu, J. Wu, S. Cui, and R. Zhu, “An energy collaboration framework considering community energy storage and photovoltaic charging station clusters,” Journal of Energy Storage, vol. 116, 2025. doi: 10.1016/j.est.2025.115976.
[17] H. Morita, H. Haga, Y. Ito, and K. Arimatsu, “Variable State of Charge-based Power Leveling Method using Multiple Energy Storage Systems,” IEEJ Journal of Industry Applications, vol. 11, no. 6, pp. 790–797, 2022. doi: 10.1541/ieeijia.22000414.
[18] X. Pan, K. Liu, J. Wang, Y. Hu, and J. Zhao, “Capacity Allocation Method Based on Historical Data-Driven Search Algorithm for

Integrated PV and Energy Storage Charging Station," Sustainability, vol. 15, no. 6, 2023. doi: 10.3390/su15065480.

[19] P. Stanko, M. Tkac, M. Kajanova, and M. Roch, "Impacts of Electric Vehicle Charging Station with Photovoltaic System and Battery Energy Storage System on Power Quality in Microgrid," Energies, vol. 17, no. 2, 2024. doi: 10.3390/en17020371.

[20] A. Szajding, M. Kuta, A. Cebo-Rudnicka, and M. Rywotycki, "Analysis of work of a thermal energy storage with a phase change material(PCM) charged with electric heaters from a photovoltaic installation," International Communications in Heat and Mass Transfer, vol. 140, 2023. doi: 10.1016/j.icheatmasstransfer.2022.106547.

[21] F. Tian, L. Huang, and C.-G. Zhou, "Photovoltaic power generation and charging load prediction research of integrated photovoltaic storage and charging station," Energy Reports, vol. 9, pp. 861–871, 2023. doi: 10.1016/j.egyr.2023.04.250.

[22] G. Cavraro, A. Bernstein, R. Carli, and S. Zampieri, "Feedback Power Cost Optimization in Power Distribution Networks With Prosumers," IEEE Transactions on Control of Network Systems, vol. 9, no. 4, pp. 1633–1644, 2022. doi: 10.1109/tcns.2022.3141028.

[23] M. Dolores Borras-Talavera, J. Carlos Bravo, and C. Alvarez-Arroyo, "Instantaneous Disturbance Index for Power Distribution Networks," Sensors, vol. 21, no. 4, 2021. doi: 10.3390/s21041348.

[24] J. Lei, Z. Yuan, H. Bai, S. Su, J. Yang, W. Li, S. Pan, and N. Liu, "Economic Dispatch of Distribution Network With Dispersed Wind Power Considering Network Reconfiguration," Frontiers in Energy Research, vol. 10, 2022. doi: 10.3389/fenrg.2022.942350.

[25] W. Li, P. Ding, W. Xia, S. Chen, F. Yu, C. Duan, D. Cui, and C. Chen, "Artificial neural network reconstructs core power distribution," Nuclear Engineering and Technology, vol. 54, no. 2, pp. 617–626, 2022. doi: 10.1016/j.net.2021.08.015.

[26] W. Liao, J. Chen, Q. Liu, R. Zhu, L. Song, and Z. Yang, "Data-driven Reactive Power Optimization for Distribution Networks Using Capsule Networks," Journal of Modern Power Systems and Clean Energy, vol. 10, no. 5, pp. 1274–1287, 2022. doi: 10.35833/mpce.2021.000033.

[27] W. Liao, D. Yang, Q. Liu, Y. Jia, C. Wang, and Z. Yang, "Data-Driven Reactive Power Optimization of Distribution Networks via Graph Attention Networks," Journal of Modern Power Systems and Clean Energy, vol. 12, no. 3, pp. 874–885, 2024. doi: 10.35833/mpce.2023.000546.

[28] S. A. Ramirez-Marin, J. Oyuela-Ocampo, and A. Garces-Ruiz, "Power aggregator in active distribution networks using IoT," Revista UIS ingenierías, vol. 22, no. 4, pp. 71–80, 2023. doi: 10.18273/revun.v22n4-2023007.

[29] S. Sepulveda, A. Garces-Ruiz, and J. Mora-Florez, "Generic optimal power flow for active distribution networks," Electrical Engineering, vol. 106, no.3, pp. 3529–3542, 2024. doi: 10.1007/s00202-023-02147-0.

[30] J. Zhao, Y. Li, J. Bai, L. Ma, C. Shi, G. Zhang, and J. Shi, "Multi-objective optimization of marine nuclear power secondary circuit system based on improved multi-objective particle swarm optimization algorithm," Progress in Nuclear Energy, vol. 161, 2023. doi: 10.1016/j.pnucene.2023.104740.

Biographies

Jian Wang, (1979–), male, wjian0805@163.com, 13885104515, senior engineer, from Guizhou Power Grid Co., LTD. Research Center for Grid Planning, Master degree. His main research direction is grid engineering consulting and evaluation.

Zhen Li, (1995–) male, master's degree, engineer, mzyclz@163.com, 18300877542, Guizhou Power Grid Co., LTD. Grid Planning and Research Center, engineer, mzyclz@163.com, 18300877542. Main research direction: demand response, new energy storage, etc.

Qingsheng Li, (1971–) male, Bachelor of Science, lqs98@126.com, 13885185953, professor-level senior engineer, main research direction: new energy storage, distribution network, power system simulation.

Yuanfeng Wang, (1980–), male, North District Branch of Guiyang Power Supply Bureau, senior engineer, bachelor's degree, 848183321@qq.com, 13608596869, main research direction: smart grid.

Ning Luo, (1986–) female, Guizhou Power Grid Co., Ltd. Power Grid Planning and Research Center, Master's degree, 547091372@qq.com, 18785069512, Senior Engineer, main research directions: distribution network planning, research on new distribution systems.